Manuscript for Annual Meeting Compendium of Papers

Quantification of the Concrete Crosstie Load Environment for Light Rail Transit Infrastructure

TRB 17-05212

Transportation Research Board 96th Annual Meeting

Submitted: August 1, 2016

Aaron A. Cook[1], J. Riley Edwards, Matthew V. Csenge, and Yu Qian

Rail Transportation and Engineering Center - RailTEC
Department of Civil and Environmental Engineering
University of Illinois at Urbana-Champaign
205 N. Mathews Ave., Urbana, IL 61801

4,962 Words, 10 Figures = 7,462 Total Word Count

Aaron A. Cook	J. Riley Edwards	Matthew V. Csenge
(970) 690-0635	(217) 244-7417	(217) 333-5768
aacook2@illinois.edu	jedward2@illinois.edu	csenge2@illinois.edu

Yu Qian
(217) 300-2131
yuqian1@illinois.edu

[1] Corresponding Author

ABSTRACT

Concrete crossties are increasingly being used in rail transit applications for a variety of performance and reliability-related reasons. While the static and dynamic loads imparted by light rail transit vehicles are lower than many other forms of rail transport (e.g. heavy rail transit, commuter rail transit, or heavy haul freight rail) in which concrete crossties are used, the need to optimize the design of these components for their loading environment remains. Additionally, little research exists on quantifying dynamic loads under revenue service operation on North American light rail systems. This paper reviews experimentation deployed on a light rail transit system to quantify in-service wheel-rail loads and crosstie bending moments in the track superstructure, and provides a summary of the results that stemmed from the instrumentation. Results include vertical rail loads, concrete crosstie center bending moments, and concrete crosstie rail seat bending moments. Vertical rail loads can inform designers of the difference between static and dynamic loads, while center negative and rail seat positive bending moments can be used in designing crossties specifically for light rail transit applications. This information is being used as part of a larger effort to design transit crossties with a mechanistic approach.

In the light rail system studied, dynamic vertical wheel loads on tangent track ranged from 5.5 to 16.7 kips (24.4 to 74.1 kN), concrete crosstie center negative bending moments ranged from 1.78 to 24.2 kip-inches (0.201 to 2.73 kNm), and concrete crosstie rail seat positive bending moments ranged from 2.88 to 50.31 kip-inches (0.326 to 5.68 kNm). While these data may not be representative of all light rail transit systems, the system studied had the 90th percentile light rail vehicle (LRV) static wheel loads.

INTRODUCTION

Concrete crossties are frequently used in rail transit applications for a variety of performance and reliability-related reasons. The static and dynamic loads imparted by light rail transit vehicles are lower than many other forms of rail transport (e.g. heavy rail transit, commuter rail transit, or heavy haul freight rail) in which concrete crossties are used, but the need to optimize their design remains. Presently, little research exists on quantifying dynamic loads under revenue service operation on North American light rail systems, critical design inputs at both the component and system level.

This paper provides results for vertical wheel-rail loads, concrete crosstie center bending moments, and concrete crosstie rail seat bending moments for the light rail transit loading environment. This research was conducted in conjunction with a larger project studying the resiliency of concrete crossties and fastening systems in North American light, heavy, and commuter rail transit systems. The overall project mission is to characterize the desired performance and resiliency requirements for concrete crossties and fastening systems, quantify their behavior under load, and develop more resilient concrete crossties and fastening system designs for rail transit operators. This design process is being approached from a mechanistic standpoint, meaning that the design starts with quantification of actual service loads, progresses to address component materials and geometry, and finally considers the system's performance as a whole. Prior work at the University of Illinois at Urbana-Champaign (UIUC) has outlined this mechanistic design process in the freight railroad domain (*1*). To begin the application of mechanistic design in the rail transit sector, a study was recently conducted to outline the static loads for light, heavy, and commuter rail systems (*2*), the data from which will be compared to the dynamic loads found in this research to generate transit mode-specific impact factors.

Accurate dynamic loading information is important in the mechanistic design of concrete crossties and fastening systems, as these loads directly influence the chosen component materials and geometric design, and both the over and under-design of these track components waste resources. Overdesign of components results in a waste of capital resources, while under design also represents waste with broken or prematurely failing components resulting in a loss of track capacity and the replacement cost of the components themselves. Since concrete crossties represent a measurable percentage of construction and maintenance costs (*3*), it is important that they are designed and manufactured for the environment in which they will be deployed.

This work represents some of the first research into quantifying the dynamic loads induced in concrete crossties in light rail transit systems (*2*), although research has already been conducted to study dynamic loading in commuter rail infrastructure using Wheel Impact Load Detector (WILD) data (*4*) and comparisons of static loads in various rail transit systems (*2*, *5*). Also, information on the factors that influence dynamic loading is included in the Track Design Handbook for Light Rail Transit (*6*), such as unsprung mass, vehicle speed, spring rate and damping of the primary and secondary suspensions, maximum operating speed, and car resonant frequency. It, does not, however, outline procedures for estimating in service dynamic loads.

Design methodologies outlined by the Track Design Handbook for Light Rail Transit (*6*) define the weights of passenger rail cars at the unloaded, fully seated passenger, fully seated passenger with average rush hour standees (4.0 Passengers/m^2 [3.3 Passengers/yd^2] of standee space), and crush (maximum occupancy or 6.0 Passengers/m^2 [5.0 Passengers/yd^2] of standee space) loads as AW0, AW1, AW2, and AW3, respectively (*7*). These loadings vary with both car type and car capacity for light, heavy, and commuter rail transit operations, and may not match international definitions due to cultural differences in rider comfort with proximity.

Recent research by UIUC to quantify static loads in North American rail transit systems used a density of 6 passengers/m^2 (5 passengers/yd^2) for AW3 loading, matching the definition provided in the Transit Capacity and Quality of Service Manual (*7*). A fifth level, AW4 or structural load, is occasionally used for bridge design but is not commonly used in the design of track superstructure components such as the crosstie and fastening systems (*6*). Using data from the National Transit Database (*8*), Lin et al. (*2*) found that there are differences in the typical static wheel loads in commuter rail from that seen on light or heavy rail transit systems. This lack of overlap from the commuter rail mode to light or heavy rail transit modes indicates that, at least within the static realm, the loading regimes are not similar. This is one reason that infrastructure constructed for a specific rail transit mode should have unique and optimized designs as the input loads are different for each mode (and, to a lesser degree, even within each mode). Results from Lin's research (Figure 1) further demonstrate that while the AW0 loads in light rail are generally lower than the AW0 loads in heavy rail, there is a large region of overlap. Specifically, almost all (99.9%) LRV AW0 wheel loads fall between 5 and 10 kips [22.2 to 44.5 kN], but this same band includes 58.5% of all heavy rail vehicles' AW0 wheel loads (*9*). All of light and heavy rail transit static wheel loads are lower than commuter rail transit wheel loads unless comparing a loaded heavy rail transit car to an unloaded commuter rail car, and both are less than commuter rail locomotive wheel loads.

The distributions shown in Figure 1 include data for 100% of LRVs, 85% of heavy rail vehicles, 72% of commuter railcars, and 91% of commuter rail locomotives operating in revenue service in the US. Figure 1 is a percent exceeding chart, meaning that the y-axis represents the percentage of sample whose magnitude exceed that on the x-axis. Each rail transit mode's line on this chart is predominately vertical, indicating that within each mode, most transit vehicles have a relatively narrow range of wheel loads. The lack of uniformity in the shapes of the AW0 and AW3 distributions is due to variation in the area available for standees on different car designs (e.g. longitudinal versus transverse seating), so the AW3 line may not be exactly the same distribution as a shifted AW0 curve.

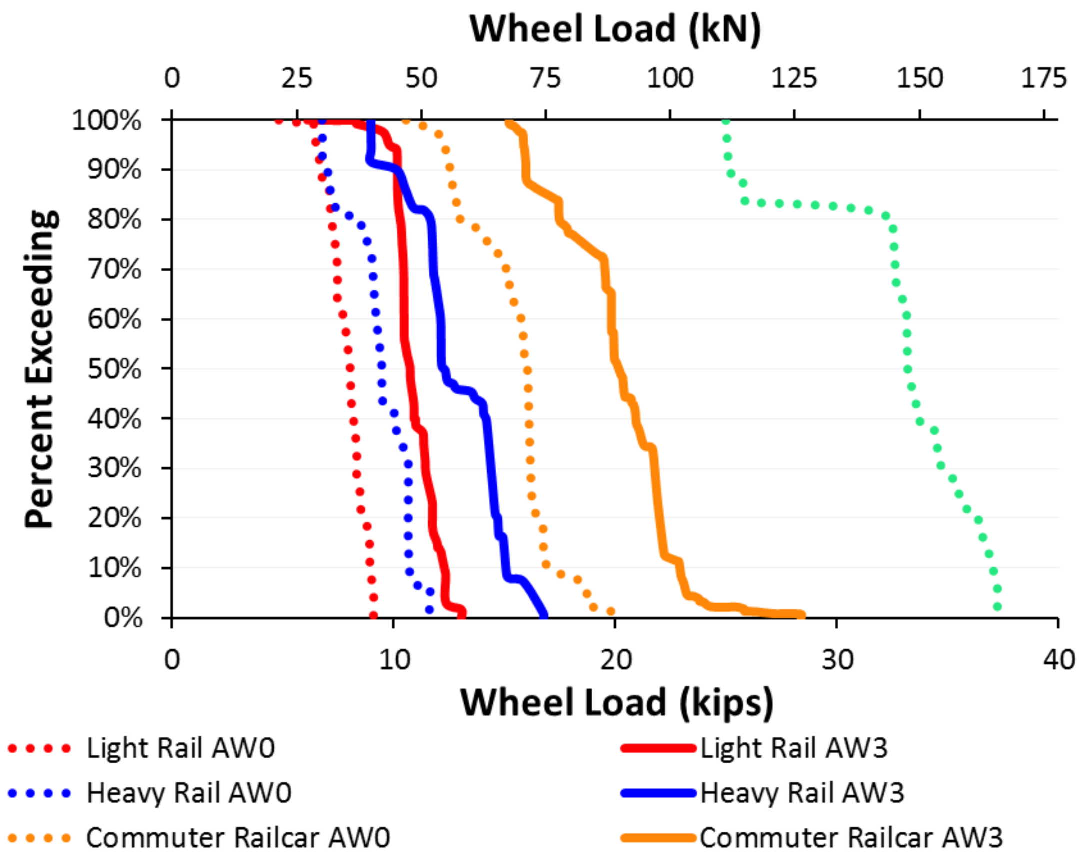

FIGURE 1 Percent exceeding values of static wheel loads for light, heavy, and commuter rail transit vehicles (*2*).

METHODOLOGY

Researchers at UIUC deployed instrumentation on St. Louis MetroLink (light rail transit provider serving the greater St. Louis, Missouri area) in March 2016 to obtain data related to the dynamic loading environment of the track superstructure under revenue service operations. Instrumentation was deployed in East St. Louis, Illinois approximately one mile west of the Fairview Heights (Illinois) station (Figure 2(a)). Instrumentation consisted of concrete crosstie surface strain gauges to measure bending moments, rail-mounted strain gauges to determine rail loads, thermocouples for measurement of temperature, and linear potentiometers for measurement of rail displacements. The aforementioned instrumentation is connected to an automated data collection system which is triggered by equipment passing a distance-measuring laser mounted trackside. All instruments, except the potentiometers which are not weather resistant, are deployed on a long-term basis and protected accordingly. The desired information from these instruments includes the loading of the track structure, the bending moments at the rail seat and the center of the concrete crosstie, and the displacements near the crosstie rail seat. An image of the instrumentation is shown in Figure 2(b), while a plan view of the instrumentation layout is shown in Figure 3. Each of the types of instrumentation are shown in Figure 4(a-e) and are described in greater depth below.

The Fairview Heights field site on St. Louis MetroLink is located on a tangent track at Milepost 23.3 on the westbound (inbound) track, the maximum allowable track speed is 55 mph (89 kph), and approximately 154 trains pass over the site each weekday.

(a) (*10*)

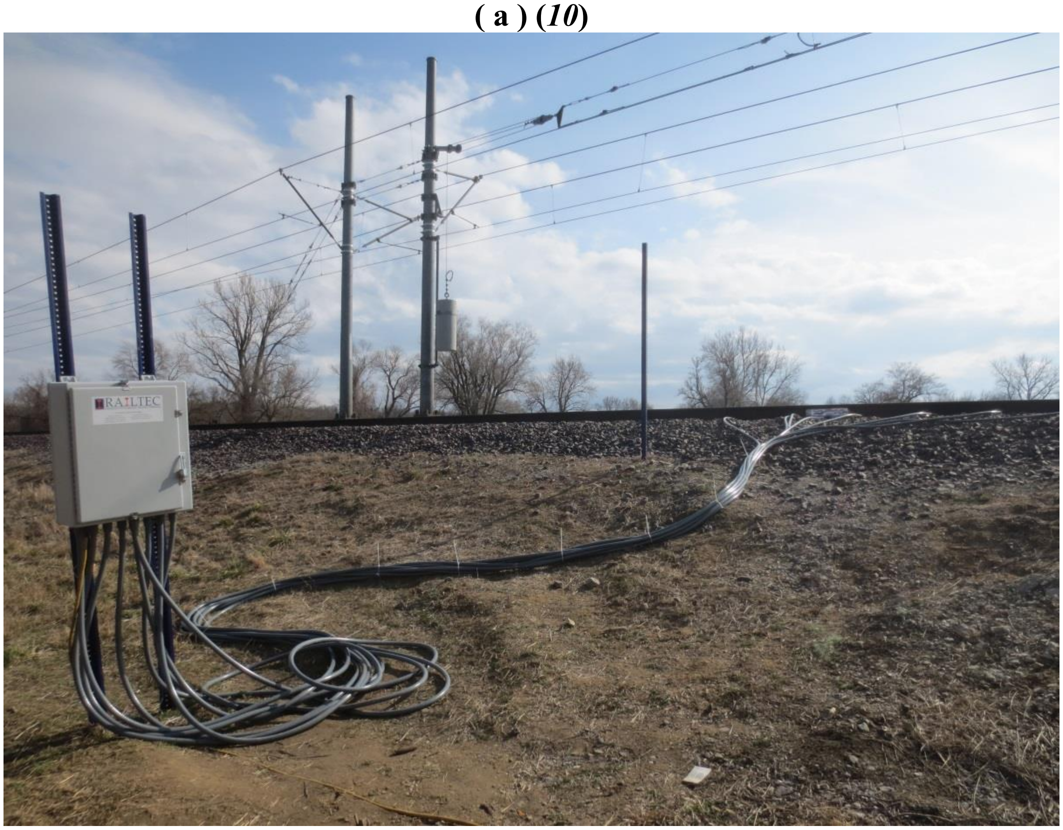

(b)

FIGURE 2 (a) Map of St. Louis MetroLink Fairview Heights, Illinois site location (b) image of the completed site showing the wayside data acquisition and transfer cabinet.

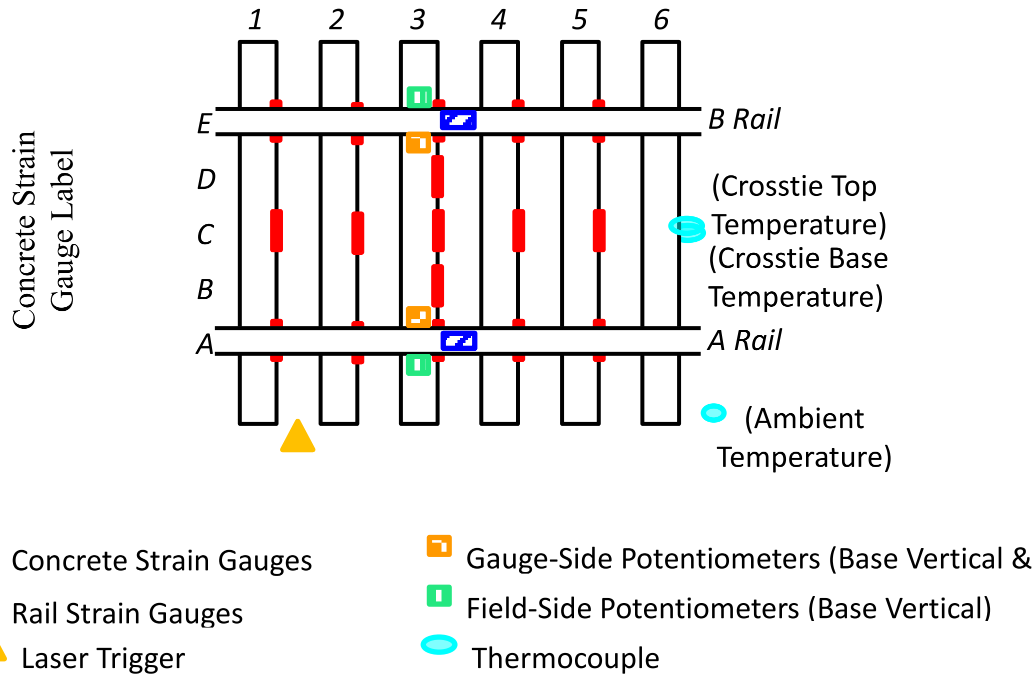

FIGURE 3 Plan view showing field instrumentation layout on St. Louis MetroLink.

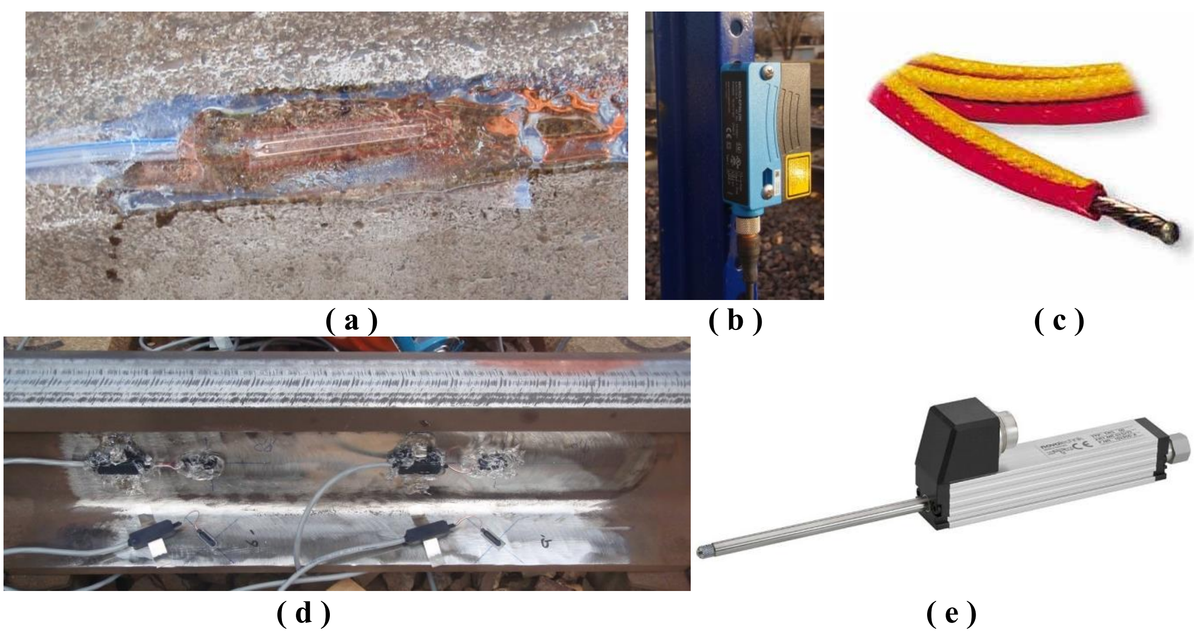

FIGURE 4 Instrumentation used at the MetroLink site: (a) concrete surface strain gauge, (b) laser-based distance measurement device, (c) thermocouple, (d) rail-mounted strain gauges, vertical (above, on rail web, with first layer of protection) and lateral (below, on rail base) (e) linear potentiometer.

Rolling Stock

St. Louis MetroLink uses Siemens SD 400 and SD 460 LRVs. These LRVs have a static empty vehicle load of 92,500 lbs. (411.46 kN), and six axles per car (*11*). This results in an average static wheel load of 7,708 lbs. (34.28 kN), though the middle truck is unpowered and the front and rear axles are powered, making some variation in the static load per wheel. This variation results in a maximum static wheel load of 9,600 lbs. (42.7 kN) and a minimum load of 6,500 lbs. (28.9 kN). St. Louis MetroLink typically operates two-car trains coupled in an AB-BA configuration, thus generating twelve axle loads per train pass.

Crosstie Flexural Behavior Measured by Concrete Surface Strain Gauges

One of the most widely accepted methods for field measurement of concrete crosstie bending moments is through the use of surface strain gauges (*1*, *12*). Concrete surface strain gauges were applied to the top chamfer of the concrete crosstie at the center of the crosstie, at the rail seat on all crossties (30 inches [76.2 cm] offset from center), and at an intermediate location halfway between the other two gauges on one crosstie (15 inches [38.1 cm] offset from center). These quarter-bridge Wheatstone strain gauges measure the strain in the crosstie, which is induced by the combination of loading on the crosstie and support conditions underneath it. Theoretically, the stresses incurred at the top chamfer could be calculated using the principles of a beam; knowing moments induced, distance from the neutral axis, and the moment of inertia of the crosstie in question can yield the stress using equation (1):

$$\varepsilon_x = -\frac{yM_z}{EI_z} \tag{1}$$

Where,

ε_x	=	the strain in the longitudinal direction (in./in.),
E	=	Young's modulus (kips/in.^{2}),
y	=	the distance from the neutral axis to the point in question (in.),
M_z	=	the moment at the point in question (kip-in.),
I_z	=	the second moment of inertia in the z-plane at the point in question (in.^{4}).

However, the cross-section of the crosstie, the location of the neutral axis, and the second moment of inertia varies along a prestressed concrete crosstie, and the actual Young's modulus of a concrete specimen varies with the quality and vintage of the concrete. As long as these qualities are not changed and the location of the strain gauge is constant, then a laboratory calibration can be used to determine the value of $-\frac{y}{EI_z}$. Knowing this value simplifies the equation, relating strain (ε_x) directly to moment (M_z) by this single calibration factor.

Crossties from the same design and vintage as those found in track at the field site were instrumented in the Research and Innovation Laboratory (RAIL) at UIUC using the same procedure and locations as the crossties in the field. Calibration was conducted using testing protocols adapted from the American Railway Engineering and Maintenance-of-Way Association (AREMA) for rail seat positive and center negative bending of a monoblock concrete crosstie, respectively (*13*). These tests applied a known moment while measuring the concrete crosstie strain at each instrumented location with the slope of this line being the $-\frac{y}{EI_z}$ term mentioned earlier. This information allows the concrete crosstie strains in the field to be divided by this term to obtain bending moments experienced by the crosstie at the points where gauges have been applied.

Wheel-Rail Interface Loads Measured by Rail Strain Gauges

Industry standard procedures of measuring wheel-rail forces such as WILDs rely on the use of rail-mounted strain gauges (*14*, *15*). Like previous UIUC research requiring input loads (*1*), rail strain gauges were applied to measure the vertical and horizontal stresses experienced by the rail, providing a measure of the input loads that are applied at the wheel-rail interface. The horizontal gauges were applied as a full Wheatstone bridge on the base of the rail and the vertical gauges were applied as a full Wheatstone bridge in the web of the rail.

Horizontal load will cause the rail to bend laterally, from which the strain of the rail is measured by the Wheatstone bridge in the base of the rail. The fixed geometry makes correlating the measured bending strain directly into load applied possible when the wheel is centered on the crib. The time which the peak vertical load is measured is taken to be the time when the wheel is centered.

The vertical load is derived from the vertical shear strains on either side of the wheel load when centered over the crib (*15*); where the reading is the sum in shear strain between the two sets of strain gauges.

The lateral and vertical Wheatstone bridges are centered between cribs with the gauges spaced 10 in. (254 mm) apart. The locations of each component of the bridges are shown in Figure 5(a), with the vertical gauges in the web of the rail and the lateral on the rail base. The distance marked "L" is the 10 in. (254 mm) separation. The wiring of each type is shown in Figure 5(b) with the lateral bridge on the left and the vertical bridge on the right.

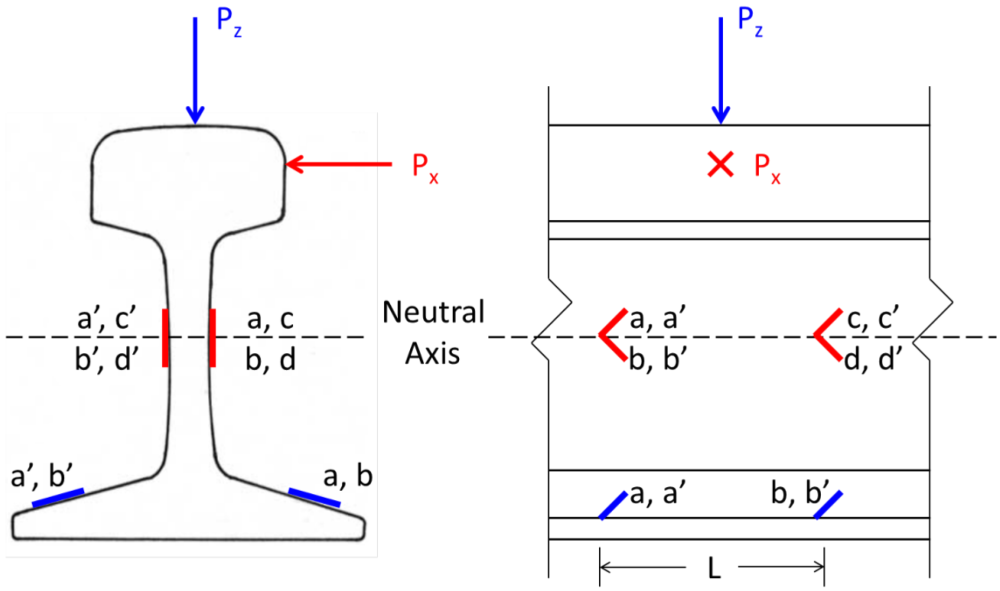

(a)

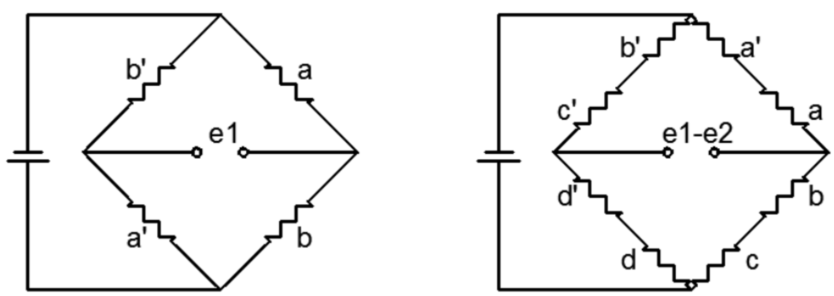

(b)

FIGURE 5 (a) Strain gauge locations and orientations on rail web and base, (b) electrical wiring for reading lateral (left) or vertical (right) gauge.

After installation, the strain bridges were calibrated on-site during a scheduled maintenance window using a “Delta Frame,” a calibrated load cell and hydraulic ram with attached reaction arms which engage against the rail to apply a known load across the strain bridges (*1*) (Figure 6). The configuration of vertical strain bridges measures shear strain at two locations and electrically finds the sum of strain. This value should be (after the modulus of the system is accounted for) the load P_z indicated in Figure 5(a). Comparing known loads applied by the Delta Frame with voltages across the strain bridges, a calibration factor can be obtained which relates voltage drop to vertical load. This calibration yields the vertical loads input into the system through the rails. The lateral strain bridge measures lateral bending strain and is more analogous to the concrete strain gauges which relate moment to load. The calibration relates the voltage drop across the bridge with the load P_x indicated in Figure 5(a).

After calibration, the vertical strain bridges yield vertical wheel-rail loads and the lateral strain bridges yield lateral wheel-rail loads. This calibration only holds true when the wheel is in the same position as the delta frame calibration occurred; that is, directly over the center point of the strain bridges, with increasing uncertainty as the wheel moves on either side. Therefore, peak values from the vertical data and the lateral reading from the same time as the vertical peak are used for each axle pass.

If enough information were known about the specifics of the entire system, as with the concrete strain gauges and Equation 1 (e.g. the modulus of elasticity and section modulus of the rail, the reactions from each crosstie, etc.), this rail response could be theoretically derived. However, applying a known load and measuring response eliminates many of the assumption errors possible with a mathematical approach.

FIGURE 6 Delta frame used to calibrate strain gauges used to determine vertical wheel-rail input loads.

The data collected from each train pass from both the rail strain bridges and concrete crosstie strain gauges were analyzed to find the peak values associated with each axle pass over each gauge. The peak value was used because it was assumed that the peak value is where the wheel load or axle pass has the greatest influence over the system. Each train pass was individually analyzed to ensure that there were not faulty gauges or data in the sample, such as when electrical noise makes distinguishing axle passes in the data difficult, or when maintenance equipment passed the site. Such data were omitted from the dataset to provide homogeneity in the dataset for the vehicles passing over the site and will be analyzed in future work.

RESULTS

After analysis of vertical loads for 561 train passes, the percent exceeding values for each rail shown were obtained (Figure 7). As can be seen in Figure 7, while there is some spread in the extreme values, there is a tight range of 50% of the measured vertical wheel loads, measuring between 7 and 9 kips (31 and 40 kN). The 99^{th}, 95^{th}, and 50^{th} percentile vertical wheel loads were 11.4, 10.2, and 8.2 kips (50.9, 45.2, and 36.5 kN), respectively. These loads are also split by axle and side in Figure 8 to show the asymmetry of the left and right sides with respect to motor locations on powered axles (axles 1, 2, 5, and 6 on each car). Within Figure 8, the boxplots represent the collected data and the lines represent the static wheel load at the time which the LRV was delivered to MetroLink. In this chart, the line in the middle of the box represents the median value, the upper and lower bounds of the box are the 75th and 25th percentile, respectively, and the whiskers (lines) extend to the last data point within 1.5 times the interquartile range past the 75th or 25th percentile value. Data outside of this range are considered outliers and are marked with "+" above or below the whisker. It should be noted that 50% of the data is within the box between the 25th and 75th percentile. Most of the variability (the range from 7 to 10 kips [31.1 to 44.5 kN]) shown in the wheel load percent exceeding chart (Figure 7) would seem to come from the different axles, not the differences in dynamic forces, because the box plot (Figure 8) shows a narrow band of loads for each wheel for the majority of data in this range, but the median values are varied within this range.

Even at the tail end of the distribution, where the highest value of wheel load was recorded at 16.7 kips (74.1 kN), this represents only 47% the expected static wheel load (35,750 lbs. [159.0 kN]) for a standard 286,000 lb. (1,272 kN) heavy haul freight car. If this load is compared to the static wheel loads for a Siemens SD 400 LRV, this represents an impact factor (as defined by AREMA) of 107%. In other words, the maximum observed dynamic load is 2.07 times the nominal static load. The 99th, 95th, and 50th percentile impact factors observed were 35%, 21%, and 0.5%, respectively. It is important to note, however, that due the nature of the installation of the rail-mounted strain gauges, only one load is obtained per wheel pass (as opposed to the entire wheel revolution at a typical WILD location (*15*)). If there is a wheel defect or dynamic forces causing the wheel to bounce, a lighter load may be recorded than that wheel is impacting further down the track.

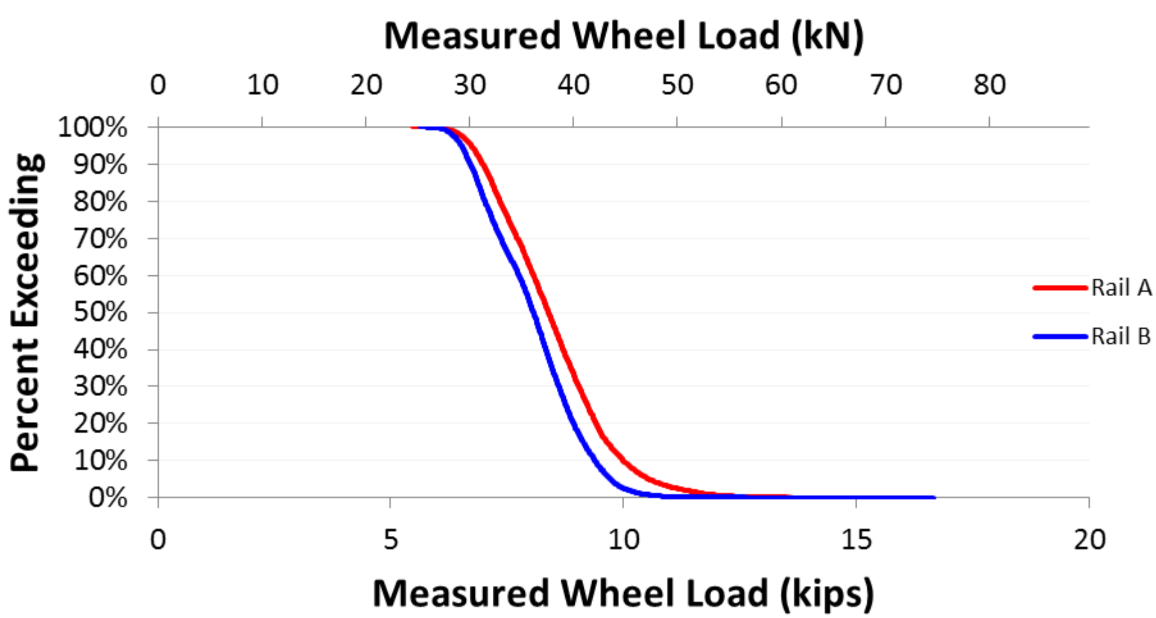

FIGURE 7 Percent exceeding values of measured wheel loads for rail a and b.

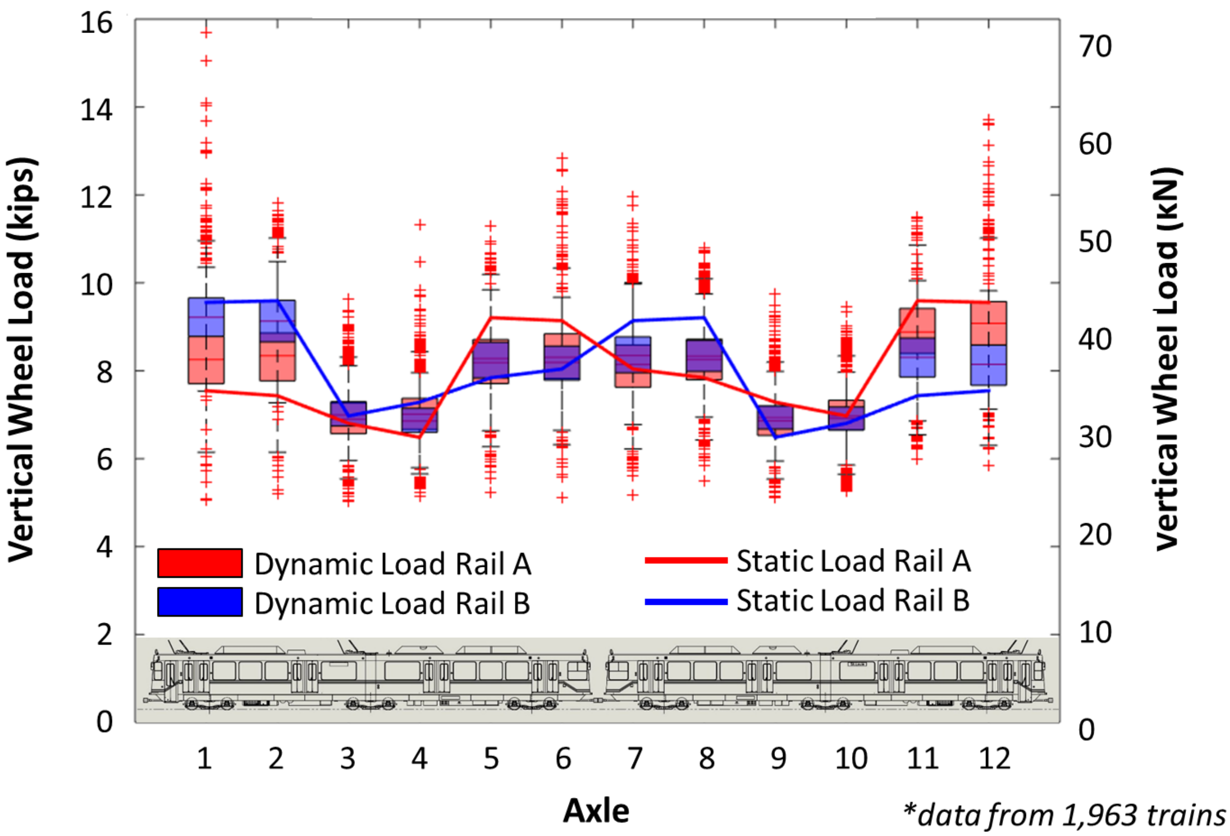

FIGURE 8 Vertical wheel loads by axle and rail, as compared to static loads provided by LRV manufacturer to St. Louis MetroLink at time of delivery.

The flexural demands on the concrete crosstie center were also plotted in terms of percentage exceeding (Figure 9). Variability exists in the sample of five crossties due to several factors. Crosstie support conditions may differ even in a short zone of five crossties, such that the bending moments are different from crosstie to crosstie. Geometric alignment of the track, though believed to be properly maintained this site, may also induce a higher dynamic load repeatedly at a location, causing the crosstie at that location to experience a higher load. However, all observed variation within any given percent exceeding band is within 5 kip-in. (0.56 kNm), which is small compared to the manufactured center negative bending capacity of the crosstie (153 kip-in. [17.3 kNm]), but quite large compared to the maximum center negative bending observed (24.2 kip-in. [2.73 kNm]). The 99th, 95th, and 50th percentile moments were 18.3, 16.8, and 11.3 kip-in. (2.06, 1.90, and 1.28 kNm), respectively.

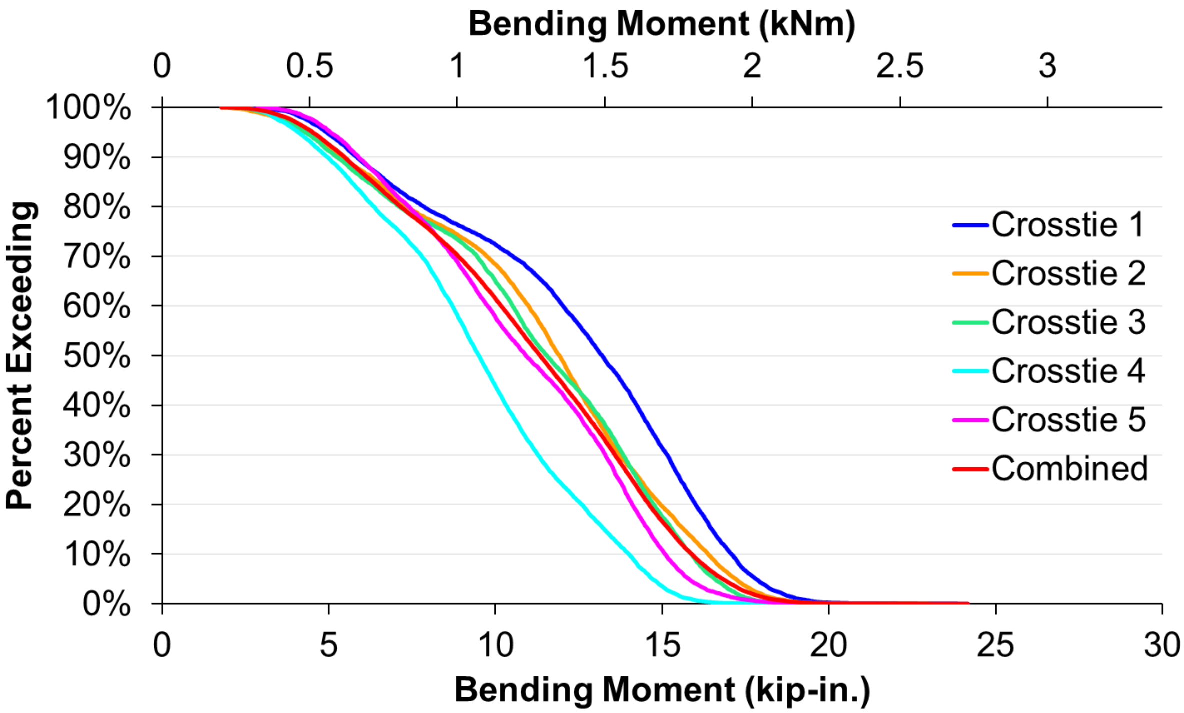

FIGURE 9 Percent exceeding values of concrete crosstie center negative bending moments, showing crosstie-to-crosstie variation in flexural demands

Rail seat positive moments are shown in Figure 10 using the same method of presentation as was previously introduced. Each rail seat is labelled by crosstie (number) and either A or E for the location of the specific rail seat. Some data indicated moments with negative bending in the rail seat on one gauge (rail seat 2E) and these moments are not shown for clarity as they represented less than 0.2% of the data collected for that gauge (or 0.02% of all data for all gauges collected), and did not surpass 37.7 kip-in. (4.26 kNm). Again, variability in the results for each rail seat observed is shown, with a higher range (in absolute terms) than that for center negative bending. The 99th, 95th, and 50th percentile moments were 32.6, 29.0, and 18.6 kip-in. (3.68, 3.28, and 2.10 kNm), respectively. The maximum rail seat positive moment measured was 50.3 kip-in. (5.68 kNm).

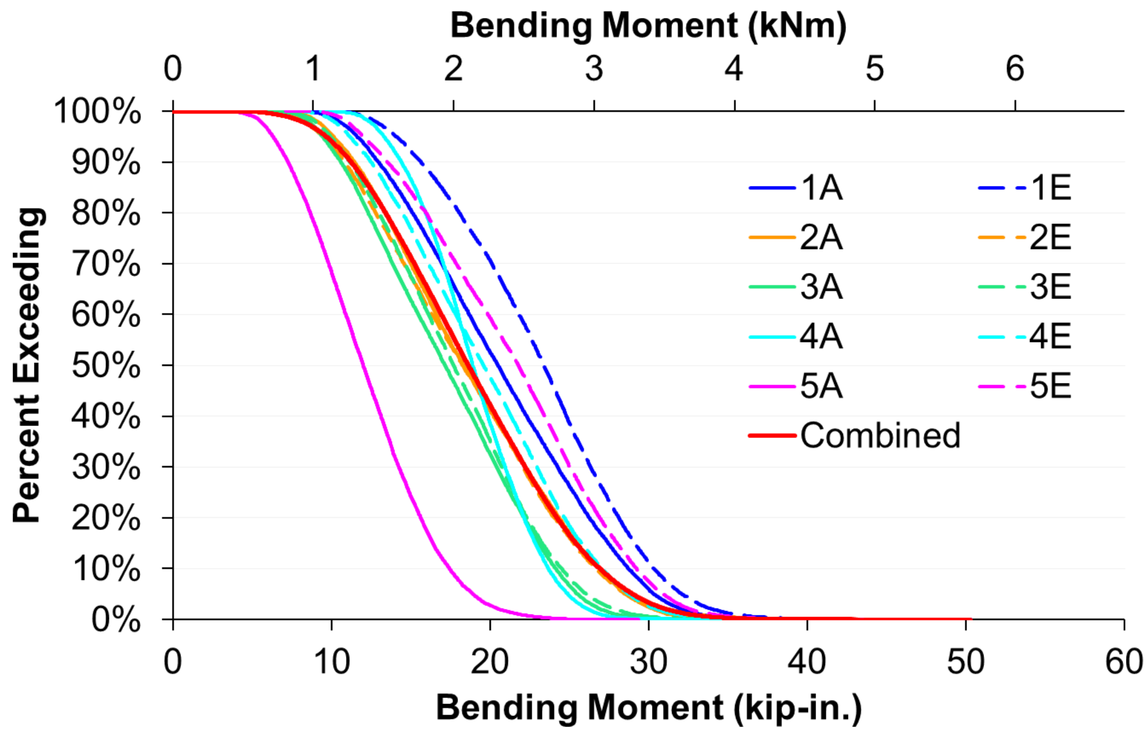

FIGURE 10 Percent exceeding values of concrete crosstie rail seat positive bending, showing variation from rail seat to rail seat

DISCUSSION

The center bending moments in crossties were analyzed and compared against typical recommended design practices and designs for an 8 foot 3 in. (2.51 meter) crosstie with 33 kip axle loads (twice the maximum recorded wheel load of 16.7 kips [74.3 kN]), and 30 in. (0.76 meter) crosstie spacing. AREMA design methodology produces a value of 99 kip-in. (11.2 kNm) (*9*, *13*), St. Louis MetroLink specifies 144 kip-in. (16.3 kNm), and the crosstie manufacturer's design specifies 153 kip-in. (17.3 kNm). The maximum center bending (24.2 kip-in. [2.73 kN-m]) observed in the trains sampled leaves 84% of the manufacturer design load unused. For normal operation of LRVs, the maximum center negative flexural demand was only 16% of the capacity of the crosstie.

For rail seat positive bending, the AREMA design methodology produces a value of 128 kip-in. (14.4 kNm) (*9*, *13*), the MetroLink specification was 179 kip-in. (20.2 kNm), and the manufacturer's design capacity is 278 kip-in. (31.4 kNm). The maximum rail seat bending (50.3 kip-in. [5.68 kNm]) observed in the trains sampled leaves 82% of the manufacturer's design load unused. For normal operation of LRVs, the maximum rail seat positive flexural demand was only 18% of the capacity of the crosstie.

In both center negative and rail seat positive bending, the maximum flexural demand found in this study (which relates to LRVs only) would need to be increased more than five times in order to reach the design capacity of the crossties' manufactured design strength. This does not necessarily mean that concrete crossties should be built to this lower load; but that the concrete crossties of traffic on transit lines with exclusive LRV traffic is likely to experience these loads or lower for the majority of their service lives given similar circumstances to the test site. The area tested was in a section of track with good maintenance and no evidence of center binding, drainage issues, alignment deviations, or other track problems, which limits the variation in support or dynamic loading for a given area. Track with these issues may be expected to have more concentrated load paths through the concrete crosstie, leading to higher flexural demands. Additionally, maintenance vehicles may have higher wheel loads than LRVs (even if they are run infrequently compared to revenue service operations), as they are often adapted from heavy-haul freight railroads with higher allowable wheel loads.

Impact Factors measure the amplification of dynamic loads over nominal static loads. AREMA recommended practice defines the impact factor as the percentage increase over nominal static load. The impact factor did not exceed 107% for a dataset of 3,073 trains, meaning that the dynamic loads were at most 2.07 times greater than the nominal static load. This is lower than the current AREMA recommended practice of using the value 200%, or loads 3 times greater than the static load (*2*, *13*).

CONCLUSION

Based on the revenue service light rail transit site instrumented for this study, design loads for crossties in light rail service have large capacity reserves when considering the movement of LRVs across the system (i.e. not the movement of maintenance of way equipment). However, further data collection and analysis needs to be conducted in regards to maintenance-of-way equipment and track construction trains, which are likely to place more demanding loads on infrastructure. This may indicate that design and implementation of a lighter duty crosstie is a feasible alternative for light rail systems, so long as considerations for the maintenance-of-way equipment, construction, and ballast trains are also made (or alternative construction techniques are developed where these are the design loads). This lighter crosstie design may lead to first cost savings, both in materials and installation.

ACKNOWLEDGEMENTS

This research was conducted as part of a larger project sponsored by the United States Department of Transportation (US DOT) Federal Transit Administration (FTA). Specific gratitude goes to St. Louis MetroLink for providing track time and flagging protection during the installation and testing of the field installation which yielded the data used in this paper, specifically Charles Clemins Jr., Brian Sellers, and Marc Cruz from MetroLink. For the overall project, additional gratitude goes to our industry partners, APTA, New York Metropolitan Transit Authority, Chicago Metra, Portland TriMet, Progress Rail Services, Amtrak, Hanson Professional Services, Pandrol USA, GIC, and LBFoster CXT Concrete Ties. J. Riley Edwards has been supported in part by grants to the UIUC Rail Transportation and Engineering Center (RailTEC) from CN, the Canadian National Railway Company; Hanson Professional Services; and the George Krambles Transportation Scholarship Fund. Aaron A. Cook has been supported in part by the CN research fellowship in railroad engineering.

REFERENCES

1. Rail Transportation and Engineering Center (RailTEC). 2015. FRA Concrete Tie and Fastener BAA Final Report. Federal Railroad Administration, Washington, D.C.
2. Lin, X., J.R. Edwards, M.S. Dersch., and C.R. Ruppert, C.R. Load Quantification for Light Rail, Heavy Rail and Commuter Rail Infrastructure. Presented at the 11th World Congress on Railway Research, Milan, Italy, 2016.

3. "M/W Budgets to Climb in 2008." *Railway Track and Structures,* Vol. 104, No. 1, 2008, pp. 18-25.
4. Sadeghi, J.M. Experimental Evaluation of Accuracy of Current Practices in Analysis and Design of Railway Track Sleepers. *Canadian Journal of Civil Engineering*, Vol. 37, No. 5, 2010, pp. 675-683.
5. Vuchic, V.R. *Urban Transit Systems and Technology*. John Wiley & Sons, Inc., New York, 2007.
6. Parsons Brinckerhoff, Inc. Track Design Handbook for Light Rail Transit, 2nd ed. Transit Cooperative Research Program, Report 155, 2012.
7. Hunter-Zaworski, K. Transit Capacity and Quality of Service Manual. Transit Cooperative Research Program Report 100, 2003, pp. 8-9
8. Federal Transit Administration (FTA), 2013 Revenue Vehicle Inventory, National Transit Database (NTD), 2013
9. Csenge, M.V., X. Lin, H.E. Wolf, M.S. Dersch and J.R. Edwards. Mechanistic Design of Concrete Monoblock Crossties for Rail Transit Loading Conditions. Presented at the American Public Transportation Association 2015 Rail Conference, Salt Lake City, UT, USA, June 2015.
10. Google. *Google Earth*. 38°36'09"N 90°03'26"W. 2016.
11. Siemens, AG. *SD460 High-Floor Light Rail Vehicle*. 2014. https://w3.usa.siemens.com/mobility/us/en/interurban-mobility/rail-solutions/high-speed-and-intercity-trains/Documents/St.Louis_DataSheet_2014_LR.pdf. Accessed 11 July 2016.
12. Wolf, H. E. *Flexural Behavior of Prestressed Concrete Monoblock Crossties*. M.S. Thesis, University of Illinois at Urbana-Champaign, 2015.
13. American Railway Engineering and Maintenance-of-Way Association. Manual for Railway Engineering. 2015.
14. Steets, P.G. and Y.H. Tse. Conrail's Integrated Automated Wayside Inspection. *Proceedings of the 1998 ASME/IEEE Joint Railroad Conference*, 1998, pp. 113-125.
15. Stratman, B., Y. Liu and S. Mahadevan. Structural Health Monitoring of Railroad Wheels Using Wheel Impact Load Detectors. *Journal of Failure Analysis and Prevention* Vol. 7, No. 3, 2007, pp. 218–225.